A method for the determination of landslide risks using a Digital Elevation Model created by Unmanned Aerial Systems with a hydrogeological data connection

Józef Sanecki, Andrzej Klewski, Marek Zygmunt⊡, Grzegorz Stępień
Roman Hałaburda, Kamil Borczyk

Maritime University of Szczecin, Faculty of Navigation, Institute of Geoinformatics
46 Żołnierska St., 71-250 Szczecin, Poland, e-mail: ig@am.szczecin.pl
⊡ corresponding author, e-mail: marek.zygmunt@op.pl

Abstract
This article presents the problem of surveying landslide prone areas. Discussed are the possibility of using photogrammetry methods for digital imaging, creating Digital Terrain Models (DTM) and Digital Elevation Models (DEM) of slope surface and combining these with the ground's angle of internal friction, cohesion and hydrogeological data. Unmanned Aerial Systems (UASs) with inclined high precision cameras show different slope angles than UASs with vertical cameras. Expressly, we can see places within the landslide area where the angle of internal friction and cohesion are low. These places are the most likely to suffer further mass movements causing fissures and ground displacements. In the observed landslide area we separated the steep parts of the slope, with low cohesion values, and the slight parts of the slope, with low values of angle of internal friction. In these different areas, landslides can evolve in different ways and at different speeds. The Factor of Safety (FS) was calculated for different types of area which allowed the probability of new mass movements to be checked for different areas. This method can be useful for C-B and X-Band PSI Interferometry Data. Because of the damage potentially incurred by landslides, there is a need to better understand these natural phenomena, especially their methods and speed of development and how they can be prevented from forming in the future.

Introduction

One of the main factors determining the growth of mass movements is the inclination of the surface. According to the "Inwentaryzacja…" (Grabowski, 2006) it is very difficult to determine the range of values for the inclinations which are most likely to result in the development of mass movements. The topic has not, to date, been examined in much depth. The important factors that help to determine the inclination angles that cause most landslides are the type of land from which the slope is built (the angle of internal friction is crucial) and the water flow systems within the slope area as well as its influence on the angle of internal friction for impermeable rocks (de Blasio, 2011). At the same time, (Van Asch, Buma & Van Beek, 1999) showed that

for shallow landslides, the slide area of the ground and rock material 1–2 m BGL is formed because of the saturation of ground that should not be subjected to saturation, with rain water. Additionally, if the angle of slope inclination is high, the ground loses its cohesion and movement of material occurs. Saturation has a bigger impact when, in addition to rain water, ground water contributes to the saturation which has a longer lasting effect on the rock-land center, if its level is too high. Water accumulated in the pores of permeable rocks minimizes the angle of internal friction of impermeable rocks that lay higher. This is the reason for the formation of deep landslides (slide area of 5–6 m BGL). Such landslides may be formed at lower angles of inclination (over a dozen degrees), where the surface saturation of rock masses is higher. In nature the most commonly

occurring situations are intermediate situations (Van Asch & Buma, 1997). A shallow landslide may be formed at a low angle of inclination that then increases the likelihood of further mass movements. Additionally, (Zydroń & Dąbrowska, 2012) showed that if the ground is characterized by increased humidity, the angle of internal friction and cohesion are reduced. However, the method of analyzing the landslides using close range photogrammetry, which allows for the precise determination of the inclination angles of the slopes and the forecasting of the formation and development of landslides, has only recently been developed. For such technology to work, it is crucial that measurements are performed with ground and airborne 3D laser scanning, with the aim of creating a uniform Digital Terrain Model (DTM), such as was the case for imaging changes within the landslide area caused by the earthquake in Taiwan in 1991 (Hsiao et al., 2004). A large number of terrain points and plenty of GPS stations allowed the disaster sites to be very precisely imaged and further deformations to be forecast. UASs are used to image the slipped land and to determine changes to the ground movement within various parts of a single landslide (Niethammer et al., 2012). The created DTMs allow the comparison of new slips to older glacial structures, enabling the tracking of the history of and forecasting further developments of a landslide. Moreover, thanks to BSL it is possible to estimate whether the mass of a building could cause a landslide (Zygmunt et al., 2017).

The goal of this publication is to propose the use of UASs for studies on active landslides, focusing on the precise determination of the angles of inclination of slopes using the high angle oblique photos gained using UASs. This allows the generation of a precise model of the terrain and the determination of any correlation with the angle of internal friction and a cohesion factor of the ground in the context of the threat of land slippage. Then, the safety factor is calculated and the landslide hazard map is generated. The method proposed by the authors may be an important supplement to, and refinement of, data gained using the Persistent Scatterer Interferometry (PSI) method which shows, both in exposed and built-up areas, very precisely, the location, course and nature of linear structures (slips and cracks) associated with sliding. The method also enables determination of the speed of the mass movements (Bianchini et al., 2015). Many of the crucial input data are obtained as point information. These are either linked to specific features (e.g. landslides, buildings) or they are sample points that are used to characterize spatial units (e.g. soil types, vegetation types). In the latter case, they need to be converted into maps through spatial interpolation using environmental correlation with landscape attributes (e.g. geostatistical interpolation methods such as co-kriging) (Zawadzki, 2005).

Study area

The studied landslide area is located in the city of Rogi-Folwark, in the municipality of Miejsce Piastowe, in the Krosno district in Poland. In morphological terms, the landslide is the right bottom of the stream valley. The stream flows into the Lubatówka river. The landslide is exposed to the south and it is 382.2 m ASL. The slope inclination is variable and falls within the following ranges: 21%, 40% and 13%. Moreover, escarpments occur on the examined slope; these are both artificial, formed by the necessary works for residential development, and natural, caused by erosion. The groundworks in the area include a gas pipeline, water supply and sanitary sewage system.

In May and June of 2010, within the examined area, shallow landslides of ground masses were formed. These caused ground dumps under the residential building on plot no. 2954 as well as on the slope and damage to the road and escarpment of the stream (Piskadło, 2010). In September 2013 the area was inventoried under the SOPO (Anti-slide system) project. It turned out, that the sliding ground mass from 2010 was part of a bigger, older landslide which was reactivated in two places. The total landslide area was then estimated as 1.19 ha (Popielski & Zygmunt, 2014). In geological terms, the landslide area is located within the area of the outer Silesian Carpathians (Oszczypko, Ślączka & Żytko, 2008). It is built of interlayers and menial layers. The rock masses are developed in the sandstone and shale facies (Frysztak-Wołkowska & Zubrzycki, 1991). The interlayers and menial layers are the southern part of the Bóbrka anticlines. Graded sandstones and slates run from NW-SE and have a dip of 7080° and azimuth of 115°. After the landslide was formed, other rock masses appeared in the area of the landslide's origin. There is a visible lithological and stratigraphic boundary between interlayers and menial layers (Popielski & Zygmunt, 2014). The overburden is built of various types of earth: sluice delusions in the form of dusty clay and compact dusty clays, clay pits, sand dusts, dusty sands and stream alluvia in the form of gravel with sandstone rubble. The thickness of the sediment-debris layer is 2.0–4.5 m.

Research method

This publication proposes the use of close range photogrammetry methods to determining landslide hazard maps. The accuracy of point determination in photogrammetric surveying mainly depends on the accuracy of the orientation of the camera during exposure, the quality of the sensor and the optical distortion associated with it as well as the exposure conditions (e.g. pressure, temperature, humidity, subject illumination, atmospheric attenuation) (Trinder & Fritz, 2008). When creating the DTM, the crucial factor is the angle of inclination of the camera during the exposure.

To create the DTM of the landslide, and to develop the digital orthophotomap, the photogrammetric flight was performed according to two perpendicular grids. For this purpose, a DJI Phantom 3 Professional UAS was used. The average attitude (above the terrain), from which the photos were taken, was 89 m. This, together with the parameters of the fixed focal length camera (3.61 mm and physical value of the pixel in the matrix (1.56 μm), allowed an average field resolution of 0.034 m to be obtained. The coverage of longitudinal and transverse images was about 90%. The photos were taken at a camera inclination angle of 80°. In this manner, 385 photos were taken and subjected to further processing. For these purposes, AgiSoft PhotoScan software was used. The research comprised the following stages:

1. Loading the photos and creating the project.
2. Spatial aerotriangulation.
3. Generating and classifying a dense cloud of points.
4. Creating a Triangulated Irregular Network (TIN) model.
5. Texturing the TIN model.
6. Creating a tiled model and texturing the dense cloud of points.
7. Generating the DTM.
8. Orthorectifying the photos.
9. Exporting the DTM and digital orthophotomap.
10. Generating the final report.

As a result of the aerotriangulation it was possible to reconstruct the external and internal orientation of the measurement sensor (non-metric camera). Determining the elements of the spatial orientation of the sensors is performed by a similarity transformation, using a three rotation matrix of the form (Kurczyński, 2014; Stępień et al., 2016):

$$\begin{bmatrix} X \\ Y \\ Z \end{bmatrix} = \begin{bmatrix} X_0 \\ Y_0 \\ Z_0 \end{bmatrix} + \lambda \begin{bmatrix} 1 & 0 & 0 \\ 0 & \cos\omega & \sin\omega \\ 0 & -\sin\omega & \cos\omega \end{bmatrix} \cdot$$

$$\cdot \begin{bmatrix} \cos\varphi & 0 & -\sin\varphi \\ 0 & 1 & 0 \\ -\sin\varphi & 0 & \cos\varphi \end{bmatrix} \begin{bmatrix} \cos\kappa & -\sin\kappa & 0 \\ \sin\kappa & \cos\kappa & 0 \\ 0 & 0 & 1 \end{bmatrix} \begin{bmatrix} x \\ y \\ z \end{bmatrix} \quad (1)$$

where:
ω – rotation around x-axis,
φ – rotation around the y-axis,
κ – rotation around the z-axis,
X, Y, Z – coordinates in a secondary system (field),
x, y, z – coordinates in a primary system (sensor),
X_0, Y_0, Z_0 – vector of translation (shift of the system),
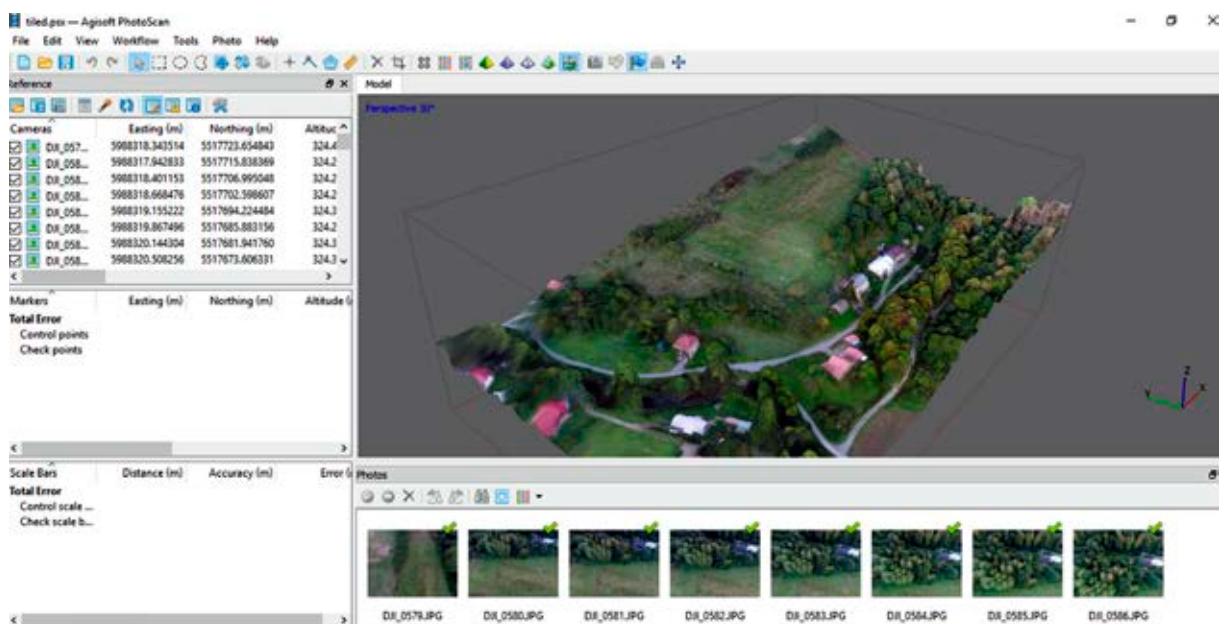λ – coefficient of scale change (in similarity transformation).

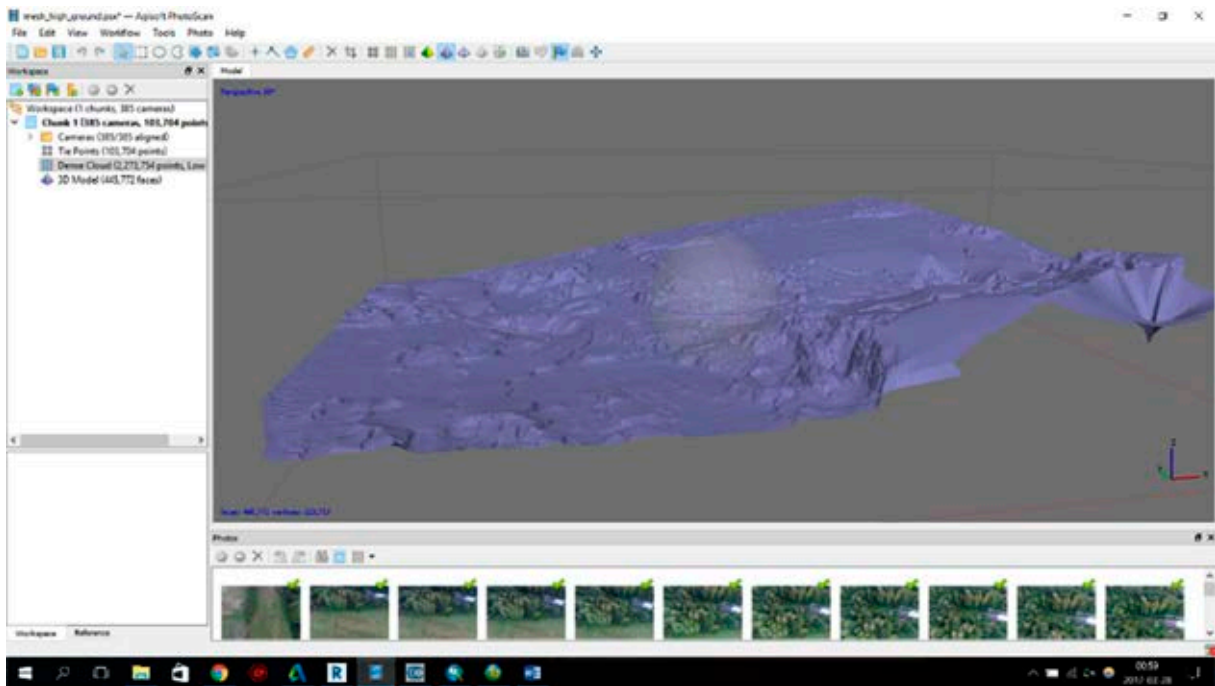**Figure 1. Generating and classifying the dense cloud of points**

Figure 2. Digital Terrain Model (DTM) created in AgiSoft PhotoScan Software

These relationships are the fundamental equations in photogrammetry because they connect the internal and external orientation elements of the measuring camera and realize the collinearity of the vectors inside and outside of the center of projections. Thus they make it possible to determine the X, Y and Z spatial coordinates in the stereoscopic coverage area of the photos.

The next stage was the creation of the dense cloud of points (Figure 1) and classifying it. At the same time, the TIN model was created and textured. The TIN model highlighted the differences in the terrain on which the landslide is located. This only shows the characteristic terrain sculpture for these types of areas.

The main escarpment of the landslide is located at 347.5 m ASL, while its tongue, which moves the stream, is located at 320 m ASL. The difference in the absolute heights within the slope area, which is part of the landslide, is 27.5 m. The vertical span of the landslide is 69.7 m. The TIN model (Figure 1) shows that the terrain in this section does not drop gently. Starting from the main escarpment and moving down the slipped area, there is a rapid fall followed by a relaxation of the slope. This is the secondary escarpment of the landslide and it was formed after its renewal because of heavy rains in 2010. The edge of the escarpment is located at a height of 340 m ASL. Below the escarpment, the heights drop suddenly to 332–330 m ASL. This small difference shows the significant undulations of the terrain and the location of the detached and clump-backed packets of clayey dust. The closer the stream, the smaller the difference. Then, ArcGIS software was used to create a map showing the variable value of the inclination angle of the slope (Figure 3).

The landslide areas shown in Figure 3 were compared to the geotechnical parameters of sandy dust obtained by (Zydroń & Dąbrowska, 2012) (Table 1). Sandy dusts are present in large quantities within the landslide's slope area in Miejsce Piastowe.

Table 1. Correlation of Geotechnical Parameters (Zydroń & Dąbrowska, 2012) with angle of Landslide Slope

Moisture content (%)	Angle of internal friction, Φ (deg)	Cohesion, c (kPa)	Landslide slope (%)
14.6	44.8	33.2	20–30 friction and cohesion
24.6	31.2	11.1	20–40 friction and cohesion
29.6	29.2	8.3	10–30 friction or 40–50 cohesion
34.6	24	8.2	0–30 friction or 40–70 cohesion

The Safety Factor (source) was estimated, in order to see which areas are most likely to suffer landslides according to the following:

$$\text{FS} = c_r + c_s + \cos^2 \alpha \left[\rho_s g (D - D_w) + (\rho_s g - \rho_w g) D_w \right]$$
$$\cdot \frac{\tan \phi}{D \rho_s g \sin \alpha \cos \alpha}$$
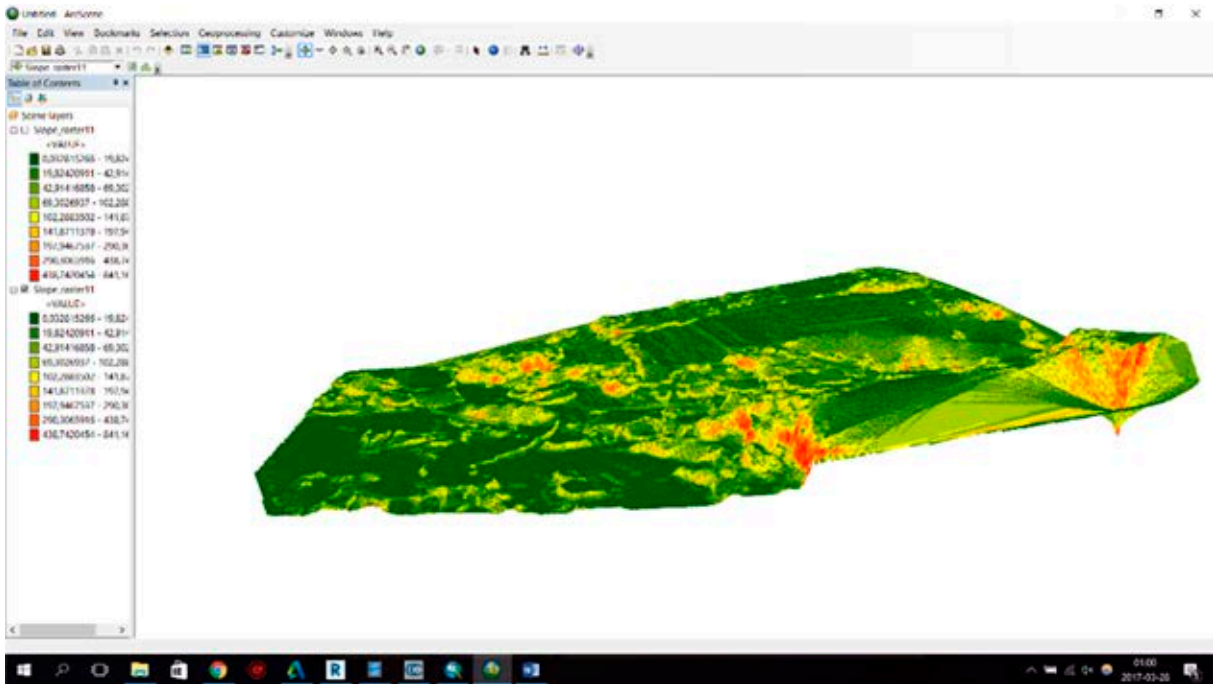
$$(2)$$

Figure 3. Digital Terrain Model (DTM) created in AgiSoft PhotoScan Software

where: c_r – root cohesion, c_s – soil cohesion, α – slope angle, D – vertical soil depth, D_w – vertical height of the water table within the soil layer, g – gravitational acceleration, ρ_s – wet soil density, ρ_w – density of water, ϕ – effective internal friction angle of the soil, r – water to soil density ratio.

For the landslide formed in the gentle part of the slope (< 30°) which was initiated by a low value of the angle of internal friction (ϕ), the value of FS was 6.83. For the landslide formed in the steep part of the slope (> 40°) which was initiated by a low value of cohesion, the value of FS was 2.52. The lower
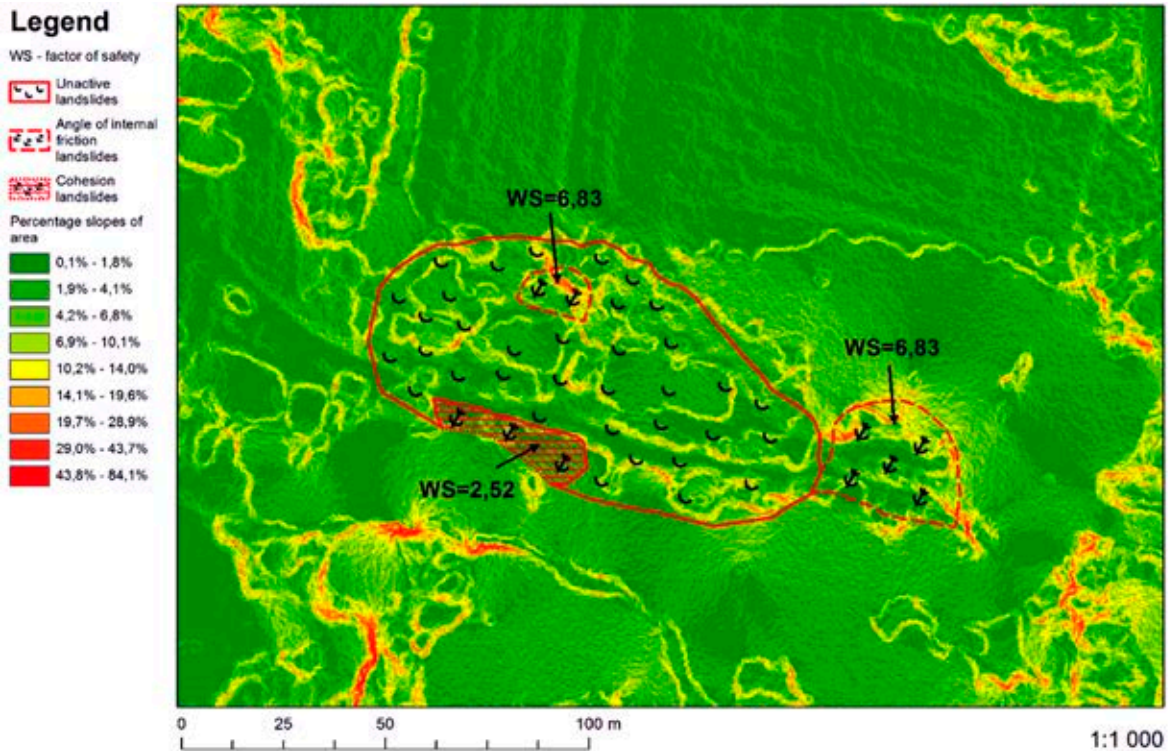

Figure 4. Landslide areas with low value angle of internal friction and low value of cohesion

the value of FS, the higher the probability of forming a landslide. The areas of gentle slope are much more stable compared to those characterized by a steep inclination. The most hazardous are the steep escarpments which are additionally cut by streams; the lower active part of the landslide is characterized by FS equal to 2.52. The central parts of the slope are safer as they are gently inclined. The upper parts of the landslide have a FS equal to 6.83.

Combining the map with the values of cohesion and angle of internal friction enables the designation of FS for the whole area (Figure 4). This allows for the classification of two active landslides, described in the introduction, into proper categories. Moreover, a previously undiscussed area, the most eastern part of the landslide could also be classified.

Discussion and conclusions

For the purposes of gaining high accuracy in imaging landslide areas, the non-metric camera was inclined to 80°. Moreover, the coverage of longitudinal and transverse images was about 90% in two perpendicular flights. The coverage of the photos was increased to the maximum, to a level that is commonly used for generating true orthophotomaps. Thanks to this solution, it was possible to look more closely at the terrain and increase the accuracy of the measured heights. In this way, the advantages of high photographic coverage and the inclined camera were utilized fully. Based on the obtained photos it was possible to generate a Digital Terrain Model of the landslide with a grid of 0.10 m hole diameter and relative vertical error ≤ 0.14 m. This enabled the precise determination of the correlations between the angle of the slope inclination, internal friction and cohesion of the ground. Thanks to these correlations, it was possible to designate the places, within the landslide area, which are likely to suffer further mass movements which could occur as a result of the low value of the angle of internal friction or low cohesion of the ground. The safety factor estimated for the areas with a low cohesion value was 2.52 and for those with a low value of internal friction angle it was 6.83. This proves the better stability of the areas located on the gentle slope ($< 30°$) compared to those on the steep slope ($> 40°$). However, it does not eliminate potential further mass movements. The most hazardous are the steep escarpments which are additionally cut by streams. The lower active part of the landslide is characterized by a safety factor equal to 2.52. The central parts of the slope are safer as they are gently inclined. The obtained data may

form an important supplement to research methods used in Persistent Scatterer Interferometry (PSI). The areas of low inclination, up to 30°, coincide with the low internal angle of the ground (freshly renovated, active slope in Miejsce Piastowe). More steep areas, characterized by low cohesion (slope inclination over 40°) are more vulnerable to single landslides (fresh landslide over the slope of the Miejsce Piastowe). On the orthophotomap, with a field resolution of 0.034 m, it can be seen that the above two landslides are part of a larger, older and inactive landslide. The damages of the municipal road are also easy to see. The combination of favorable hydro-geological conditions, appropriate geo-technical parameters and slope angle were the direct cause of landslide activation. Performing two perpendicular flights, with the camera inclined at 80° and maximizing the coverage of longitudinal and transverse images to 90%, enabled higher accuracy when determining the slope inclinations. The high absolute and relative accuracy of the points allows for the extensive use of close range photogrammetry methods; in particular, the use of UASs, for determining the slope angles within a landslide and showing the correlations between the slope angle and the internal friction angle and cohesion. Consequently, it is possible to estimate the safety factor and develop a precise (spatial) landslide hazard map, which was the purpose of this research.

Acknowledgments

References

1. BIANCHINI, S., CIAMPALINI, A., RASPINI, F., BARDI, F., DI TRAGLIA, F., MORETTI, S. & CASAGLI, N. (2015) Multi-Temporal Evaluation of Landslide Movements and Impacts on Buildings in San Fratello (Italy) by Means of C-Band and X-Band PSI Data. *Pure and Applied Geophysics* 172 (11), pp. 3043–3065.
2. de BLASIO, F.V. (2011) *Introduction to the Physics of Landslides. Lecture notes on the dynamics of mass wasting.* Springer Netherlands.
3. FRYSZTAK-WOŁKOWSKA, A. & ZUBRZYCKI, A. (1991) *Objaśnienia do Szczegółowej mapy geologicznej Polski w skali 1:50000 ark. Rymanów (1040).* Warszawa: CAG Państwowy Instytut Geologiczny – Państwowy Instytut Badawczy.
4. GRABOWSKI, D. (2006) *Inwentaryzacja osuwisk oraz zasady i kryteria wyznaczania obszarów predysponowanych do występowania i rozwoju ruchów masowych w Polsce Pozakarpackiej.* Warszawa: CAG Państwowy Instytut Geologiczny – Państwowy Instytut Badawczy.

5. Hsiao, K.H., Liu, J.K., Yu, M.F. & Tseng, Y.H. (2004) *Change detection of landslide terrains using Ground-Based Lidar data*. XXth ISPRS Congress, Istanbul, Turkey, Commission VII, WG VII/5, 5p.

6. Kurczyński, Z. (2014) *Fotogrametria*. Warszawa: Wydawnictwo PWN.

7. Niethammer, U., James, M.R., Rothmund, S., Travelletti, J. & Joswig, M. (2012) UAV-based remote sensing of the Super-Sauze landslide: Evaluation and results. *Engineering Geology* 128 (1), pp. 2–11.

8. Oszczypko, N., Ślączka, A. & Żytko, K. (2008) Regionalizacja tektoniczna Polski. Karpaty zewnętrzne i zapadlisko przedkarpackie. *Przegląd Geologiczny* 10, pp. 927–935.

9. Piskadło, R. (2010) *Ekspertyza Geotechniczna dla ustalenia geotechnicznych warunków posadowienia drogi gminnej i budynku mieszkalnego nr 151 po naruszeniu stateczności zbocza osuwiskami w miejscowości Rogi, gmina – Miejsce Piastowe*. Zespół Usług Geologiczno-Technicznych „HGS-EKO". Krosno, ul. Czajkowskiego 55.

10. Popielski, W. & Zygmunt, M. (2014) *Objaśnienia do Mapy Osuwisk i Terenów Zagrożonych Ruchami Masowymi w skali 1:10000 dla gminy Miejsce Piastowe*. Warszawa: CAG Państwowy Instytut Geologiczny – Państwowy Instytut Badawczy.

11. Stępień, G., Sanecki, J., Klewski, A. & Beczkowski, K. (2016) Wyznaczanie granic użytków rolnych z wykorzystaniem bezzałogowych systemów latających. *Infrastruktura i ekologia terenów wiejskich, Infrastucture and Ecology of Rural Areas* III/2, pp. 1011–1024.

12. Trinder, J. & Fritz, L.W. (2008) Historical development of ISPRS. In: Li, Z. Chen, J. & Baltsavias, E. (Eds) *Advances in Photogrammetry, Remote Sensing and Spatial Information Sciences: 2008 ISPRS Congress Book*, pp. 3–20.

13. Van Asch, Th.W.J. & Buma, J. (1997) Modelling groundwater fluctuations and the frequency of movement of a landslide in the Terres Noires region of Barcellonnette (France). *Earth Surface Processes and Landforms* 22 (2), pp. 131–141.

14. Van Asch, Th.W.J., Buma, J. & Van Beek, L.P.H. (1999) A view on some hydrological triggering systems in landslides. *Geomorphology* 30 (1–2), pp. 25–32.

15. Zawadzki, J. (2005) *Wykorzystanie metod geostatystycznych w badaniach środowiska przyrodniczego*. Prace Naukowe Politechniki Warszawskiej. Inżynieria Środowiska.

16. Zydroń, T. & Dąbrowska, J. (2012) The influence of moisture content on shear strength of cohesive soils from the landslide area around Gorlice. *AGH Journal of Mining and Geoengineering* 36 (2), pp. 309–317.

17. Zygmunt, M., Stępień, G., Sanecki, J., Klewski, A. & Beczkowski, K. (2017) Określanie wpływu masy zabudowy na powstawanie osuwisk przy wykorzystaniu bezzałogowych systemów latających. *Infrastruktura i ekologia terenów wiejskich, Infrastucture and Ecology of Rural Areas* (In preparation).